Eur. Phys. J. A **21**, 479–486 (2004)
DOI 10.1140/epja/i2004-10012-2

THE EUROPEAN PHYSICAL JOURNAL A

High-energy hadron spin-flip amplitude at small momentum transfer and new A_N data from RHIC

J.-R. Cudell[1,a], E. Predazzi[2,b], and O.V. Selyugin[1,c]

[1] Institut de Physique, Bât. B5a, Université de Liège, Sart Tilman, B-4000 Liège, Belgium
[2] Dipartimento di Fisica Teorica, Università di Torino and Sezione INFN di Torino, Torino, Italy

Received: 9 January 2004 / Revised version: 17 March 2004 /
Published online: 14 September 2004 –
Communicated by A. Schäfer

Abstract. In the case of elastic high-energy hadron-hadron scattering, the impact of the large-distance contributions on the behaviour of the slopes of the spin–non-flip and of the spin-flip amplitudes is analysed. It is shown that the long tail of the hadronic potential in impact parameter space leads to a value of the slope of the reduced spin-flip amplitude larger than that of the spin–non-flip amplitude. This effect is taken into account in the calculation of the analysing power in proton-nucleus reactions at high energies. It is shown that the preliminary measurement of A_N for p ^{12}C obtained by the E950 Collaboration indeed favours a spin-flip amplitude with a large slope. Predictions for A_N at $p_L = 250$ GeV/c are given.

PACS. 13.85.Dz Elastic scattering – 13.85.Lg Total cross sections – 13.85.-t Hadron-induced high- and super-high-energy interactions (energy > 10 GeV)

1 Introduction

Diffractive polarised experiments open a new window on the spin properties of QCD at large distances. In particular, the recent data from RHIC and HERA indicate that, even at high energy, the hadronic amplitude has a significant spin-flip contribution, $\mathcal{A}^{\rm h}_{\rm sf}$, which remains proportional to the spin–non-flip part, $\mathcal{A}^{\rm h}_{\rm nf}$, as energy is increased. There were many observations of spin effects at high energies and at fixed momentum transfers. Several attempts to extract the spin-flip amplitude from the experimental data show that the ratio of spin-flip to spin–non-flip amplitudes can be non-negligible and may be only slightly dependent on energy [1–3]. Thus, the diffractive polarised experiments at HERA and RHIC allow one to study spin properties of quark-pomeron and proton-pomeron vertices and to search for a possible odderon contribution. This provides an important test of the spin properties of QCD at large distances. In all of these cases, pomeron exchange is expected to contribute to the observed spin effects at some level [4].

In the framework of perturbative QCD, it was shown that the analysing power of hadron-hadron scattering can be non-negligible and proportional to the hadron mass [5]. Hence, one would expect a large analysing power for moderate p_t^2, where the spin-flip amplitudes are presumably relevant for diffractive processes. When large-distance contributions are considered, one obtains a more complicated spin structure for the pomeron coupling. For example, the spin-flip amplitude has been estimated in the QCD Born approximation by the non-relativistic quark model for the nucleon wave function [6] in the case where the nucleon contains a dynamically enhanced component with a compact di-quark. The spin-flip part of the scattering amplitude can be determined by the hadron wave function for the pomeron-hadron couplings or by the gluon-loop corrections for the quark-pomeron coupling [7]. As a result, the spin asymmetries that appear have a weak energy dependence as $s \to \infty$. Additional spin-flip contributions to the quark-pomeron vertex may also have their origin in instantons (see, *e.g.*, [8,9]).

The inclusion in the analysis of the experimental data on spin-correlation parameters does not simplify the task. In the general case, the form of the analysing power, A_N, and the position of its maximum, depend on the parameters of the elastic-scattering amplitude, *i.e.* $\sigma_{\rm tot}$, $\rho(s,t)$, the Coulomb-nucleon interference phase $\varphi_{\rm CN}(s,t)$ and the elastic slope $B(s,t)$. For the definition of new effects at small angles, and especially in the region of the diffraction minimum, one must know the effects of the Coulomb-hadron interference with sufficiently high accuracy. The Coulomb-hadron phase was calculated in the entire

[a] e-mail: J.R.Cudell@ulg.ac.be
[b] e-mail: predazzi@to.infn.it
[c] On leave from the Bogoliubov Laboratory of Theoretical Physics, JINR, 141980, Dubna, Moscow Region, Russia; e-mail: selugin@qcd.theo.phys.ulg.ac.be

diffraction domain taking into account the form factors of the nucleons [10]. Some polarisation effects connected with the Coulomb-hadron interference, including some possible odderon contribution, were also calculated [11].

The dependence of the hadron spin-flip amplitude on momentum transfer at small angles is tightly connected with the basic structure of the hadrons at large distances. We shall show that the slope of the "reduced" hadron spin-flip amplitude (the hadron spin-flip amplitude without the kinematic factor $\sqrt{|t|}$) can be larger than the slope of the hadron spin–non-flip amplitude, as was observed long ago [12,13]. This leads to small effects in the differential hadron cross-section and in the real part of the hadron spin–non-flip amplitude [14].

The new RHIC fixed-target data, from E950, consist in measurements of the analysing power

$$A_N(t) = \frac{\sigma^{(\uparrow)} - \sigma^{(\downarrow)}}{\sigma^{(\uparrow)} + \sigma^{(\downarrow)}} \tag{1}$$

for momentum transfer $0 \leq |t| \leq 0.05$ GeV^2, for a polarised p beam hitting a (spin-0) ^{12}C. In this region of t, the electromagnetic amplitude is of the same order of magnitude as the hadronic amplitude, and the interference of the imaginary part of $\mathcal{A}^{\rm h}_{\rm nf}$ with the spin-flip part of the electromagnetic amplitude $\mathcal{A}^{\rm em}_{\rm sf}$ leads to a peak in the analysing power A_N, usually referred to as the Coulomb-Nuclear Interference (CNI) effect [15–17]. This effect was observed in the data from [18], but the errors were too big to draw any conclusion on the hadron spin-flip amplitude.

The first RHIC measurements at $p_L = 22$ GeV/c [19] in p^{12}C scattering indicated, however, that A_N may change sign already at very small momentum transfer. Such a behaviour cannot be described by the CNI effect alone. Indeed, fits to the data [20] give for

$$r_5 = \lim_{t\to 0}\ \tilde{\mathcal{A}}^{\rm h}_{\rm sf}/{\rm Im}(\mathcal{A}^{\rm h}_{\rm nf}) \equiv R + iI\,, \tag{2}$$

$$R = 0.088 \pm 0.058\,, \quad I = -0.161 \pm 0.226\,. \tag{3}$$

2 Ratio of slopes of spin-flip and spin–non-flip amplitudes

As usual,

$$\tilde{\mathcal{A}}_{\rm sf}(s,t) \equiv 2\ m_p\ \mathcal{A}_{\rm sf}(s,t)/\sqrt{|t|}$$

is the "reduced" spin-flip amplitude, factoring out trivial kinematic factors. The large error on ${\rm Im}(r_5)$ unfortunately leads to a high uncertainty on the size of the hadronic spin-flip amplitude.

For spin-(1/2) scattering, the total helicity amplitudes can be decomposed in sub-amplitudes describing the ways the two spins can be changed during the collision:

$$\Phi_i(s,t) = \phi^{\rm h}_i(s,t) + \phi^{\rm em}_i(t)\exp[i\alpha_{\rm em}\varphi_{\rm CN}(s,t)], \quad i = 1,\ 5,$$

where $\phi^{\rm h}_i(s,t)$ represents the pure strong interaction of hadrons, $\phi^{\rm em}_i(t)$ represents their electromagnetic interaction, $\alpha_{\rm em} = 1/137$ is the electromagnetic constant, and $\varphi_{\rm CN}(s,t)$ is the electromagnetic-hadron interference phase factor. So, to determine the hadron spin-flip amplitude at small angles, one should take into account all electromagnetic and all electromagnetic-hadronic interference effects.

In this paper, as we shall be interested in scalar targets, we define the spin–non-flip amplitudes as $\mathcal{A}^{\rm h}_{\rm nf}(s,t) = (\phi^{\rm h}_1(s,t) + \phi^{\rm h}_3(s,t))/(2s)$ for the hadronic one, and $\mathcal{A}^{\rm c}_{\rm nf}(s,t) = (\phi^{\rm em}_1(s,t) + \phi^{\rm em}_3(s,t))/(2s)$ for the electromagnetic one. Taking into account the Coulomb-nuclear phase $\varphi_{\rm CN}$, we obtain ${\rm Im}\mathcal{A}^{\rm c}_{\rm nf} \approx \alpha_{\rm em}\varphi_{\rm CN}|\mathcal{A}^{\rm c}_{\rm nf}|$. The "reduced" spin-flip amplitudes are denoted as $\tilde{\mathcal{A}}^{\rm h}_{\rm sf}(s,t) = \phi^{\rm h}_5(s,t)/(s\sqrt{|t|})$ and $\tilde{\mathcal{A}}^{\rm c}_{\rm sf}(s,t) = \phi^{\rm em}_5(s,t)/(s\sqrt{|t|})$.

As usual, we define the slopes B_i of the scattering amplitudes as the derivatives of the logarithm of the amplitudes with respect to t. For an exponential form of the amplitudes, this coincides with the standard slope of the differential cross-sections divided by 2. If we define the forms of the separate hadron scattering amplitude as

$$\begin{aligned} &{\rm Im}\mathcal{A}_{\rm nf}(s,t) \sim \exp(B^+_1 t), \quad {\rm Re}\mathcal{A}_{\rm nf}(s,t) \sim \exp(B^+_2 t),\\ &{\rm Im}\tilde{\mathcal{A}}_{\rm sf}(s,t) \sim \exp(B^-_1 t), \quad {\rm Re}\tilde{\mathcal{A}}_{\rm sf}(s,t) \sim \exp(B^-_2 t), \end{aligned} \tag{4}$$

then, at small t (in $[0, 0.1]$ GeV^2), almost all phenomenological analyses assume $B^+_1 \approx B^+_2 \approx B^-_1 \approx B^-_2$. To obtain this, we can take the eikonal representation for the scattering amplitude

$$\begin{aligned} \phi^{\rm h}_1(s,t) &= -ip\int_0^\infty \rho\ {\rm d}\rho\ J_0(\rho q)[e^{\chi_0(s,\rho)}\ -\ 1],\\ \phi^{\rm h}_5(s,t) &= -ip\int_0^\infty \rho\ {\rm d}\rho\ J_1(\rho q)\ \chi_0(s,\rho)\ e^{\chi_0(s,\rho)}, \end{aligned} \tag{5}$$

where p is the momentum in the centre-of-mass frame, $q = \sqrt{-t}$ is the momentum transfer, and $\chi_i(s,\rho)$ are the eikonal phases in impact parameter (ρ) space coming from the spin–non-flip ($i = 1$) and spin-flip interaction ($i = 2$) potentials $V_i(\rho, z)$. If the potentials V_i are assumed to have the same Gaussian form, in the first Born approximation, $\phi^{\rm h}_1$ and $\hat{\phi}^{\rm h}_5$ will also have the same Gaussian form

$$\begin{aligned} \phi^{\rm h}_1(s,t) &\sim \int_0^\infty \rho{\rm d}\rho J_0(\rho q)e^{-\rho^2/2R^2} = R^2 e^{R^2 t/2},\\ \hat{\phi}^{\rm h}_5(s,t) &\sim \frac{1}{q}\int_0^\infty \rho^2{\rm d}\rho J_1(\rho q)e^{-\rho^2/(2R^2)} = R^4 e^{R^2 t/2}. \end{aligned} \tag{6}$$

In this special case, the slopes of the spin-flip and "residual" spin–non-flip amplitudes are indeed the same.

However, a Gaussian form of the potential is at best adequate to represent the central part of the hadronic interaction. This form cuts off the Bessel function and the contributions at large distances. If we expand the $J_i(x)$ at small x and truncate the series at order x^2, we obtain

$$J_0(x) \simeq 1 - (x/2)^2 \quad \text{and} \quad 2\,J_1/x\ \simeq\ (1\ -0.5\,(x/2)^2), \tag{7}$$

and the corresponding integrals

$$\phi_1^{\rm h}(s,t) \sim \int_0^\infty \rho {\rm d}\rho \left(1-\rho^2\frac{q^2}{4}\right) e^{-\rho^2/2R^2} \approx R^2 e^{-R^2\ q^2/2},$$
$$\hat{\phi}_5^{\rm h}(s,t) \sim \frac{1}{q}\int_0^\infty \rho^2 {\rm d}\rho\rho\frac{q}{2}\left(1-\rho^2\frac{q^2}{8}\right) e^{-\rho^2/2R^2}$$
$$\approx R^4 e^{-R^2q^2/2}. \quad (8)$$

still have the same behaviour over q^2 [21]. So, the integral representation for spin-flip and spin–non-flip amplitudes will be the same as in (6).

If, however, the potential (or the corresponding eikonal) has a long (exponential or power) tail in impact parameter, the approximation (7) for the Bessel functions does not lead to correct results and one has to perform the full integration.

Let us examine the contribution of large distances. The Hankel asymptotics of the Bessel functions at large distances [22] are

$$J_\nu(z) = \sqrt{2/\pi z}\,[P(\nu,z)\ \cos\chi(\nu,z) - Q(\nu,z)\ \sin\chi(\nu,z)],$$
$$P(\nu,z) \sim \sum_{k=0}^\infty (-1)^k\ \frac{(\nu,\ 2k)}{(2z)^{2k}},$$
$$Q(\nu,z) \sim \sum_{k=0}^\infty (-1)^k\ \frac{(\nu,\ 2k+1)}{(2z)^{2k+1}},$$
$$\chi(\nu,z) = z-(\nu/2+1/4). \quad (9)$$

This gives for $\nu = 0,\ 1$

$$J_0(x) = \sqrt{2/(\pi x)}[P_0(x)\cos(x-\pi/4) - Q_0(x)\sin(x-\pi/4)],$$
$$J_1(x) = \sqrt{2/(\pi x)}[P_1(x)\cos(x-3\pi/4) - Q_1(x)\sin(x-3\pi/4)], \quad (10)$$

with

$$P_0(x) \approx 1-0.0703125/x^2+0.1121521/x^4+\dots,$$
$$Q_0(x) \approx -0.125/x+0.073242188/x^3+\dots,$$
$$P_1(x) \approx 1+0.1171875/x^2-0.144195557/x^4+\dots,$$
$$Q_1(x) \approx 0.375/x-0.10253906/x^3+\dots. \quad (11)$$

From this, we obtain

$$\sqrt{\pi x}J_0(x) \approx \left(1-\frac{0.125}{x}-\frac{0.07}{x^2}\right)\cos x + \left(1+\frac{0.125}{x}-\frac{0.07}{x^2}\right)\sin x,$$
$$\sqrt{\pi x}J_1(x) \approx \left(1+\frac{0.375}{x}+\frac{0.117}{x^2}\right)\sin x - \left(1-\frac{0.375}{x}+\frac{0.117}{x^2}\right)\cos x. \quad (12)$$

The leading behaviour at large x will thus be proportional to $1/\sqrt{q\rho}$.

Let us calculate the corresponding integrals in the case of large distances

$$\phi_1^{\rm h}(s,t) \sim \int_1^\infty \rho^2/\sqrt{q\ \rho}\ \ \exp[-\rho^2/(2R^2)]\ {\rm d}\rho = 1/\sqrt{2\ q}\ \ R^{3/2}\ \gamma[3/4;1/(2R^2)],$$
$$\phi_5^{\rm h}(s,t)/q \sim 1/q\ \int_0^\infty \rho^2/\sqrt{q\ \rho}\ \ \exp[-\rho^2/(2R^2)]\ {\rm d}\rho = 1/(q\ \sqrt{q})\ \ 2^{1/4}\ \ R^{5/2}\ \ \gamma[5/4;1/(2R^2)], \quad (13)$$

where $\gamma[a;z]$ is the incomplete Gamma-function. We see that the exponential asymptotics of both representations are the same, but the reduced spin-flip amplitude has an additional $q^{3/2}$ in the denominator and hence it has a larger effective slope then the spin–non-flip amplitude. Slightly more complicated calculations, keeping the $O(1/x)$ in (12), lead to practically the same results:

$$\phi_1^{\rm h}(s,t) \sim 1/q^2\int_0^\infty \sqrt{x}\left[\left(1-\frac{0.125}{x}\right)\cos x + \left(1+\frac{0.125}{x}\right)\sin x\right]e^{-x^2/(2R^2q^2)}{\rm d}x$$
$$\approx \frac{R}{q}\ {}_1F_1(3/4,1/2,-q^2R^2/2),$$
$$\frac{\phi_5^{\rm h}(s,t)}{q} \sim \frac{1}{q^4}\int_0^\infty x^{3/2}\ \left[\left(\frac{0.375}{x}-1\right)\cos x + \left(1-\frac{0.375}{x}\right)\sin x\right]e^{-x^2/(2R^2q^2)}\ {\rm d}x$$
$$\approx \frac{R^{3/2}}{q^{5/2}}\ {}_1F_1(3/4,1/2,-q^2R^2/2). \quad (14)$$

Again, the additional $q^{3/2}$ in the denominator leads to a larger slope for the residual spin-flip amplitude. So, despite the fact that the integrals have the same exponential behaviour asymptotically, the additional inverse power of q leads to a larger effective slope for the residual spin-flip amplitude, although we take a Gaussian representation in impact parameter.

These results can be confirmed by a numerical calculation of the relative contributions of the large distances. We calculate the scattering amplitude in the Born approximation in the cases of exponential and Gaussian form factors in impact parameter representations as a function of the upper limit b of the corresponding integral

$$\phi_1^{\rm h}(t) \sim \int_0^b\ \rho\ {\rm d}\rho\ J_0(\rho\Delta)f_n,$$
$$\phi_5^{\rm h}(t)/q \sim \int_0^b\ \rho^2\ {\rm d}\rho\ J_1(\rho\Delta)\ f_n \quad (15)$$

with $f_n = \exp[-(\rho/5)^n]$, and $n = 1,\ 2$. We then calculate the ratio of the slopes of these two amplitudes $R_{BB} = B^{\rm sf}/B^{\rm nf}$ as a function of b for these two values of n. The result is shown in fig. 1. We see that at small impact parameter the value of R_{BB} is practically the same

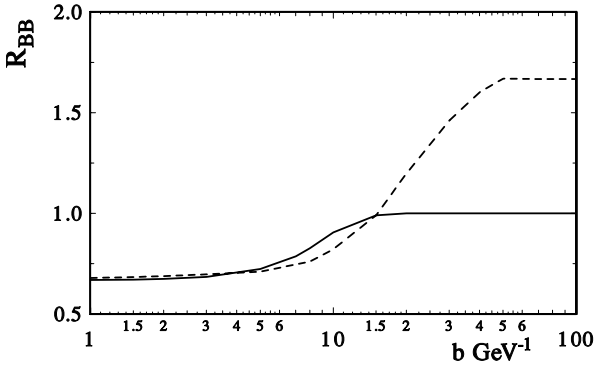

Fig. 1. The ratio of the effective slopes R_{BB} for the cases $n = 1$ (dashed line) and $n = 2$ (solid line) as a function of the upper bound of the integrals b.

in both cases and depends weakly on the value of b. However, at large distances, the behaviour of R_{BB} is different. In the case of the Gaussian form factor, the value of R_{BB} reaches its asymptotic value ($= 1$) quickly. But in the case of the exponential behaviour, the value R_{BB} reaches its limit $R_{BB} = 1.7$ only at large distances. These calculations confirm our analytical analysis of the asymptotic behaviour of these integrals at large distances.

The first observation that the slopes do not coincide was made in [12]. It was found from the analysis of the $\pi^{\pm}p \to \pi^{\pm}p$ and $pp \to pp$ reactions at $p_L = 20$–30 GeV/c that the slope of the "residual" spin-flip amplitude is about twice as large as the slope of the spin–non-flip amplitude. This conclusion can also be reached from the phenomenological analysis carried out in [13] of spin correlation parameters in elastic proton-proton scattering at $p_L = 6$ GeV/c.

In [21], it was shown that in the case of an exponential tail for the potentials $\chi_i(b,s) \sim He^{-a\rho}$, and using the standard integral representation

$$\int_0^\infty x^{\alpha-1} \exp(-p\,x) J_\nu(cx)\,\mathrm{d}x = I_\nu^\alpha,$$

with $I_\nu^{\nu+2} = 2p\,(2c)^\nu\,\Gamma(\nu+3/2)/[\sqrt{\pi}(p^2+c^2)^{3/2}]$, one obtains

$$\mathcal{A}_{\rm nf}(s,t) \sim \frac{1}{a\sqrt{a^2+q^2}}\, e^{-Bq^2},$$
$$\tilde{\mathcal{A}_{\rm sf}}(s,t) \sim \frac{3\,a\,B^2}{\sqrt{a^2+q^2}}\, e^{-2\,Bq^2}. \qquad (16)$$

In this case, one can see that the slope of the "residual" spin-flip amplitude exceeds the slope of the spin–non-flip amplitudes by a factor of two.

It is interesting to note that the derivative relations for the helicity amplitudes with $t \neq 0$ and $\{\lambda_i\} = \lambda_c, \lambda_d, \lambda_a, \lambda_b$, $\Delta\lambda = |\lambda_c - \lambda_d - \lambda_a + \lambda_b|$ for spin-dependent amplitudes, carefully examined in [23],

$$F_{\lambda_i}(s,t) = C_{\lambda_i}(s)\left(\sqrt{-t}\right)^{\Delta\lambda}\left(\frac{1}{\sqrt{-t}}\frac{\partial}{\partial\sqrt{-t}}\right)^{\Delta\lambda} F_{\Delta\lambda=0}(s,t) \qquad (17)$$

lead to the same results. In the case of a Gaussian form for the spin–non-flip amplitude, using (17), we obtain the same slopes for the spin-flip and spin–non-flip amplitudes. But if we choose another t-dependence for the spin–non-flip amplitude, for example that given by the hadronic form factor $\Lambda^2/(\Lambda^2 - t)^n$, the spin-flip amplitude is then given by

$$F_{1/2,-1/2}(s,t) = C_{1/2,-1/2}(s)\sqrt{-t}\frac{\Lambda^2}{(\Lambda^2-t)^{n+1}}. \qquad (18)$$

In the case $n = 1$, the slope becomes about twice as large. The same result was obtained in the impact parameter representation in [21]. Of course, the derivative relations at non-asymptotic energy should be used with care, as was done for the derivative dispersion relations for forward scattering [24].

Hence, a long-tail hadronic potential implies a significant difference in the slopes of the "residual" spin-flip and of the spin–non-flip amplitudes. Note also that the procedure of eikonalization will lead to a further increase of the difference between these two slopes.

3 The analysing power in proton-nucleus scattering

The above results can be used in the description of the analysing power at small momentum transfer. In the case of hadron-hadron scattering at large energy, the experimental data are scarce. The most famous experiment on proton-proton scattering at $p_L = 200$ GeV/c has large errors, and the analysis of [2] concludes that the hadron spin-flip amplitude contributes very little. Of course, it will be very interesting to obtain further measurements from the RHIC PP2PP Collaboration. At present, we only have preliminary experimental data on A_N in proton-carbon elastic scattering. Despite the fact that these data have bad normalisation conditions, the form of the analysing power is already very interesting.

For p^{12}C scattering, the elastic and total cross-sections, and the analysing power A_N, are given by

$$\begin{aligned} \mathrm{d}\sigma/\mathrm{d}t &= \pi\left(|\mathcal{A}_{\rm nf}|^2 + |\mathcal{A}_{\rm sf}|^2\right), \\ \sigma_{\rm tot} &= 4\pi\,\mathrm{Im}(\mathcal{A}_{\rm nf}), \\ A_N\,\mathrm{d}\sigma/\mathrm{d}t &= -2\pi\,\mathrm{Im}\left(\mathcal{A}_{\rm nf}\mathcal{A}_{\rm sf}^*\right). \end{aligned} \qquad (19)$$

Each term includes a hadronic and an electromagnetic contribution: $\mathcal{A}_i(s,t) = \mathcal{A}_i^{\rm h}(s,t) + \mathcal{A}_i^{\rm em}(t)e^{i\delta}, (i = {\rm nf}, {\rm sf})$, where $\mathcal{A}_i^{\rm h}(s,t)$ describes the strong interaction of p with ^{12}C, and $\mathcal{A}_i^{\rm em}(t)$ their electromagnetic interaction. $\alpha_{\rm em}$ is the electromagnetic fine structure constant, and the Coulomb-hadron phase δ is given by $\delta = Z\alpha_{\rm em}\varphi_{\rm CN}$ with Z the charge of the nucleus, and $\varphi_{\rm CN}$ the Coulomb-nuclear phase [10]. The electromagnetic part of the scattering amplitude can be written as

$$\mathcal{A}_{\rm nf}^{\rm em} = \frac{2\alpha_{\rm em}\,Z}{t}\,F_{\rm em}^{^{12}{\rm C}}F_{\rm em1}^{p}, \qquad (20)$$
$$\mathcal{A}_{\rm sf}^{\rm em} = -\frac{\alpha_{\rm em}\,Z}{m_p\sqrt{|t|}}\,F_{\rm em}^{^{12}{\rm C}}F_{\rm em2}^{p},$$

where $F^p_{\rm em1}$ and $F^p_{\rm em2}$ are the electromagnetic form factors of the proton, and $F^{^{12}{\rm C}}_{\rm em}$ that of ^{12}C. We use

$$F^p_{\rm em1} = \frac{4m_p^2 - t(\kappa_p+1)}{(4m_p^2-t)(1-t/0.71)^2}, \tag{21}$$

$$F^p_{\rm em2} = \frac{4m_p^2\kappa_p}{(4m_p^2-t)(1-t/0.71)^2}, \tag{22}$$

where m_p is the mass of the proton and κ_p its anomalous magnetic moment. We obtain $F^{^{12}{\rm C}}_{\rm em}$ from the electromagnetic density of the nucleus

$$D(r) = D_0 \left[1+\tilde{\alpha}\left(\frac{r}{a}\right)^2\right] e^{-\left(\frac{r}{a}\right)^2}. \tag{23}$$

$\tilde{\alpha} = 1.07$ and $a = 1.7$ fm give the best description of the data [25] in the small-$|t|$ region, and produce a zero of $F^{^{12}{\rm C}}_{\rm em}$ at $|t| = 0.130$ GeV^2. We also calculated $F^{^{12}{\rm C}}_{\rm em}$ by integration of the nuclear form factor given by a sum of Gaussians [26] and obtained practically the same result with the zero now at $|t| = 0.133$ GeV^2.

We now need to model the strong-interaction parts of the amplitude. Isoscalar targets such as ^{12}C simplify the calculation as they suppress the contribution of the isovector reggeons ρ and a_2, by some power of the atomic number. Also, as ^{12}C is spin 0, there are only two independent helicity amplitudes: proton spin-flip and proton spin–non-flip. However, nuclear targets lead to large theoretical uncertainties because of the difficulties linked to nuclear structure, and of the lack of high-energy proton-nucleus scattering experiments (see, for example, [27]).

For the t-dependence, as we shall be concerned with the small-t region, we shall assume that they are well approximated by falling exponentials. The slope parameter $B(s,t)/2$ is then the derivative of the logarithm of the amplitude with respect to t. If one considers only one contribution to the amplitude, this corresponds with the slope $B(s,t)$ of the differential cross-section.

Specific questions appear when we consider the energy dependence of the spin–non-flip and spin-flip amplitudes and their phase, or their ratios ρ of real to imaginary parts.

For the latter, the situation is not settled. Firstly, we may expect the size of ρ^{pA} to be $\rho^{pA} = \rho^{pp}/2$, as the a_2 and ρ contributions decrease in the nucleus. Secondly, experimental data on proton-deuteron [28] however show practically the same size for $\rho^{p{\rm D}}$ and ρ^{pp}, from which we might conclude[1] that $|\rho_{pn}| \leq |\rho_{pp}|$. Thirdly, ref. [32] shows that $|\rho_{pp}| > |\rho_{p{\rm D}}| > |\rho_{p{\rm He}}|$, and leads to the conclusion that the size of ρ depends on the atomic number with $\rho_{pA} \simeq \rho_{pp}/A$. In this case, we obtain for p^{12}C scattering at large energies $\rho \approx 0$. Finally, the data from [34,37] indicate that it is very likely that $\rho^{pA} \geq 0$.

In this paper, we choose an intermediate variant:

$$\rho_{p^{12}{\rm C}} \approx \rho_{pp}/2, \tag{24}$$

which corresponds to $\rho_{pA} = \rho_{pp}A^{-1/3}$. We emphasise that we do not know the energy dependence of ρ^{pA}, but because the ρ and a_2 trajectories are suppressed in proton-carbon scattering, and because they contribute negatively, it must be larger than in the pp case, where it is about -0.1 in this energy region.

The energy dependence of the asymptotic spin-flip amplitude is also far from decided. As mentioned above, it is possible that, in high-energy hadron-hadron scattering, the ratio of the spin–non-flip to the spin-flip amplitude decreases slowly with energy. In this case, if we take only the asymptotic part of the spin-flip amplitude into account, we cannot make its real part proportional to ρ_{pp}. In the following, we shall see that imposing proportionality to ρ_{pp} leads to a strong energy dependence for the spin-flip amplitude.

The above considerations lead to the following form for the hadron spin–non-flip amplitude:

$$\mathcal{A}^{pA}_{\rm nf}(s,t) = (1+\rho^{pA})\frac{\sigma^{pA}_{\rm tot}(s)}{4\pi}\exp\left(\frac{B^+}{2}t\right). \tag{25}$$

The slope and ρ-parameter are assumed to be proportional to their values in pp scattering, which we take as in [37]:

$$\begin{aligned} B^+_{pp}(s) &= 11.13 - 6.21/\sqrt{p_L} - 0.3\ \ln p_L, \\ \rho^{pp}(s) &= 6.8/p_L^{0.742} - 6.6/p_L^{0.599} + 0.124. \end{aligned} \tag{26}$$

The total cross-sections were chosen as

$$\sigma^{pA}_{\rm tot} = R_{{\rm C}/p}(s)\sigma^{pp}_{\rm tot}\,. \tag{27}$$

The pp total cross-section is obtained from the best form of [33], which works well in this energy region:

$$\begin{aligned} \sigma^{pp}_{\rm tot}(s) = 35.9 + 0.316\ \log^2\frac{s}{s_0} \\ +42.1\left(\frac{s}{s_1}\right)^{-0.468} - 32.2\left(\frac{s}{s_1}\right)^{-0.540}, \end{aligned} \tag{28}$$

with all coefficients in mb, $s_1 = 1$ GeV^2 and $s_0 = 34.41$ GeV^2. The analysis of [35] and the data of [36] show that the ratio $R_{{\rm C}/p}$ decreases very slowly in the region $5 \leq p_L \leq 600$ GeV/c. So, we take

$$R_{{\rm C}/p}(s) = 9.5\ (1 - 0.015\ln s) \tag{29}$$

for the energy region $24 \leq p_L \leq 250$ GeV/c.

The experiment data [37] on pC scattering at $p_L = 600$ GeV/c gives us $B^+_{p{\rm C}}(t \approx 0.02\ {\rm GeV}^2) = 62\ {\rm GeV}^{-2}$. But the experiment data [34] on hadron-nucleus scattering gives at small t $B^+_{p{\rm C}}(t \approx 0.01\ {\rm GeV}^2) = 70.5\ {\rm GeV}^{-2}$ at $p_L = 70$ GeV/c, and $B^+_{p{\rm C}}(t \approx 0.01\ {\rm GeV}^2) = 74\ {\rm GeV}^{-2}$ at

[1] The analysis based on partial-wave amplitudes and dispersion relations [29] leads qualitatively to the same result. Note that this analysis works well at low energies, but that it has some problems at high energies. For example, the values of $\rho(p\bar{p})$ from [30] seem to conflict with recent data [31]. This may be due to the fact that the data on which one must rely for such a study sometimes contradict each other, mainly because ρ is not a direct observable, but requires some theoretical input which varies from one experiment to the other.

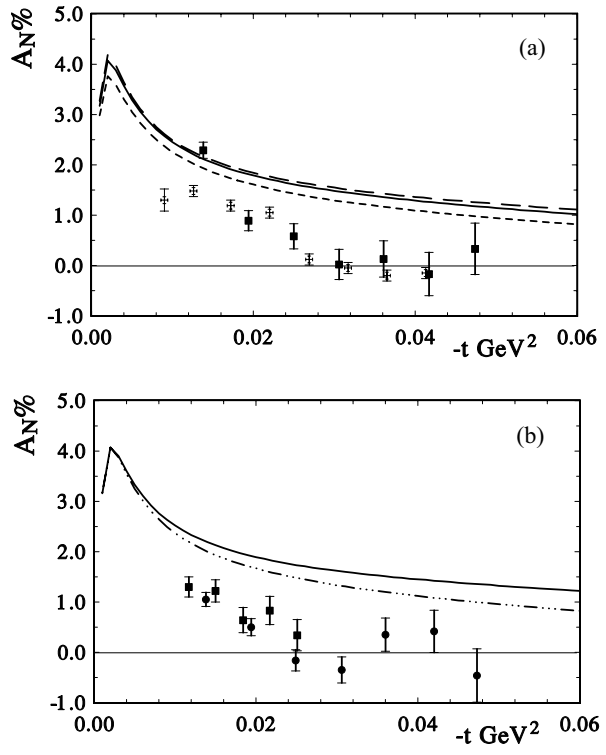

Fig. 2. (a) The energy dependence of A_N (without hadron spin-flip) at $p_L = 24,\ 100,\ 250$ GeV/c (dashed, solid, and long-dashed lines, correspondingly) compared with the data at $p_L = 22$ GeV/c (crosses) and $p_L = 24$ GeV/c (boxes) [19, 38] (only statistical errors are shown). (b) The dependence of A_N (without hadron spin-flip) over B^+ (solid line: B^+ is normalised to the data of [34]; dash-dots: B^+ is normalised to the data of [37]) compared with the data at $p_L = 100$ GeV/c (boxes and circles) [38] (only statistical errors are shown).

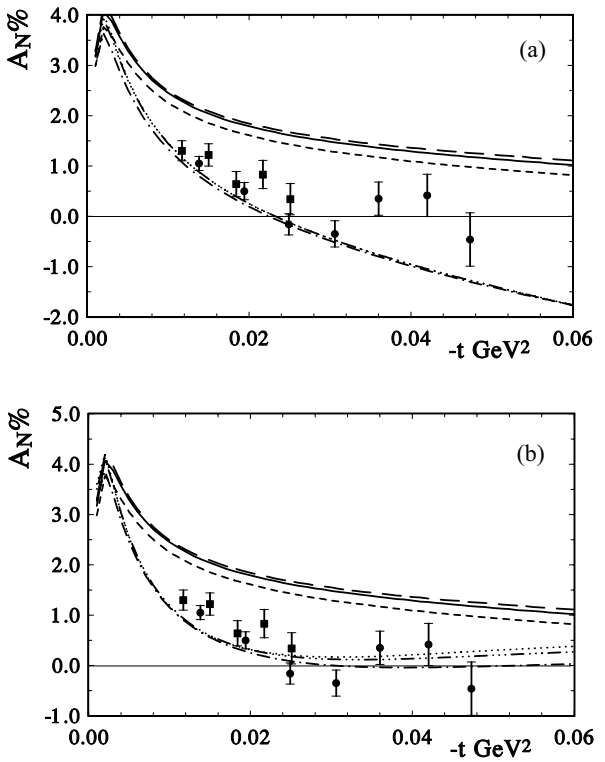

Fig. 3. (a) A_N with hadron spin-flip amplitude in case I ($B^- = B^+$) for $p_L = 24$ GeV/c (dash-dot) and $p_L = 100, 250$ GeV/c (dash-dots), compared with the curves of fig. 2(a). (b) A_N with hadron spin-flip amplitude in case II ($B^- = 2B^+$) for $p_L = 24,\ 100,\ 250$ GeV/c. (dash-dot, dash-dots, and dots, correspondingly), compared with the curves of fig. 2(a).

$p_L = 175$ GeV/c. Hence, we assume that the slope slowly rises with $\ln s$ in a way similar to the pp case, and normalise it so that it reproduces [34] or [37]. These two normalisations give us a slope of similar value $B^+_{p\mathrm{C}} \simeq 5.5\ B_{pp}$.

We can now parameterize the spin-flip part of p^{12}C scattering as

$$\mathcal{A}^{\mathrm{h}}_{\mathrm{sf}}(s,t) = (k_2\ +\ i\ k_1)\frac{\sqrt{|t|}\ \sigma^{pA}_{\mathrm{tot}}(s)}{4\pi}\exp\left(\frac{B^-}{2}t\right). \quad (30)$$

According to the above analysis, we investigate two extreme cases for the slope of the spin-flip amplitude:

- case I: the spin-flip and the spin–non-flip amplitude have the same slope $B^-_{p\mathrm{C}} = B^+_{p\mathrm{C}}$;
- case II: $B^-_{p\mathrm{C}} = 2B^+_{p\mathrm{C}}$.

One could of course allow for more freedom and try to determine the values of the slope B^-, but the data are not yet precise enough to do this. The coefficients k_1 and k_2 are chosen to obtain the best description of A_N at $p_L = 24$ and 100 GeV/c. Of course, we can only aim at a qualitative description as the data are only preliminary and as they are normalised to those at $p_L = 22$ GeV/c [19].

From the full scattering amplitude, the analysing power is given by

$$A_N\frac{\mathrm{d}\sigma}{\mathrm{d}t} = -4\pi[\mathrm{Im}(\mathcal{A}_{\mathrm{nf}})\mathrm{Re}(\mathcal{A}_{\mathrm{sf}}) - \mathrm{Re}(\mathcal{A}_{\mathrm{nf}})\mathrm{Im}(\mathcal{A}_{\mathrm{sf}})], \quad (31)$$

each term having electromagnetic and hadronic contributions.

Now, let us first calculate A_N without the contribution of the hadron spin-flip amplitude. In this case, the size and shape of A_N are determined by the interference between the hadron spin–non-flip amplitude and the magnetic part of the electromagnetic amplitude. In fig. 2(a), the results of such calculations are shown for small momentum transfer, at $p_L = 24,\ 100,\ 250$ GeV/c, and are compared with the preliminary data at $p_L = 22,\ 24$ GeV/c [19,38]. The energy dependence is weak and is determined mostly by the energy dependence of ρ, which we have taken proportional to ρ_{pp}. In fig. 2(b), the calculations are made at $p_L = 100$ GeV/c for the different normalisations of the slope. These lead respectively, at $p_L = 100$ GeV/c, to the values $B^+_{p\mathrm{C}} = 58.3$ GeV^{-2} and $B^+_{p\mathrm{C}} = 72.1$ GeV^{-2}. It is clear that this difference only slightly changes the size of A_N at $|t| \geq 0.02$ GeV^2.

In fig. 3, we show the values of A_N calculated for cases I and II for the slope of the hadron spin-flip amplitude. We can see that in both cases we obtain a small energy

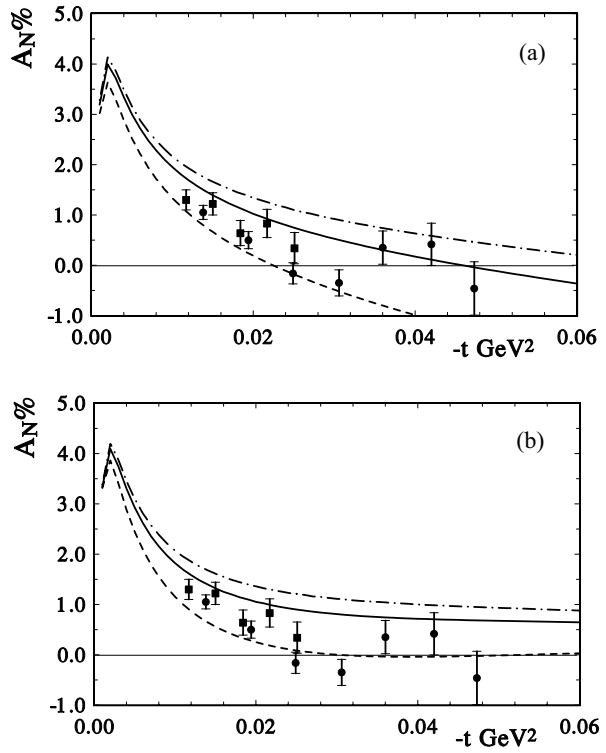

Fig. 4. A_N with a hadron spin-flip amplitude which has an additional energy factor $\sqrt{s_1}/\sqrt{s}$. (a) In case I ($B^- = B^+$) for $p_L = 24, 100, 250$ GeV/c. (dashed, solid, and dash-dotted line, correspondingly). (b) The same in case II ($B^- = 2B^+$).

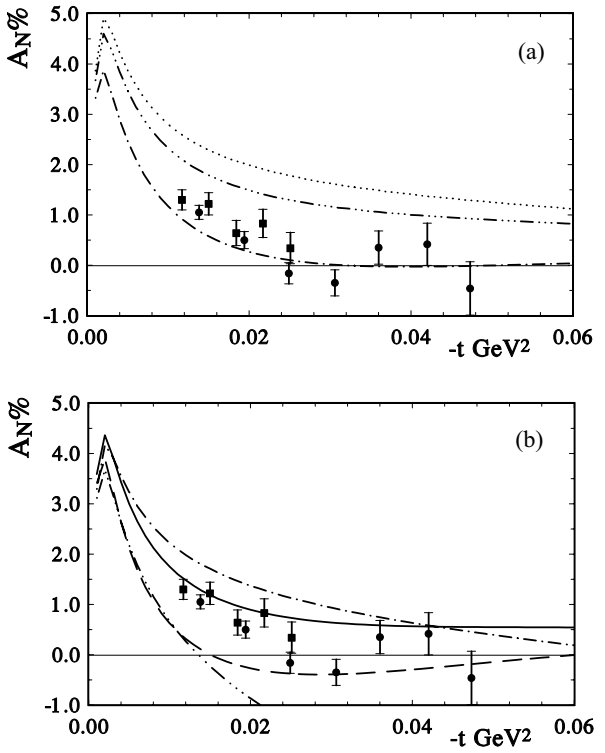

Fig. 5. (a) A_N in case II ($B^- = 2B^+$) and with the real part of the spin-flip amplitude proportional to ρ at $p_L = 24,\ 100,$ and 250 GeV/c. (dash-dot, dash-dots, and dots, correspondingly). (b) The values of A_N corresponding to a change of ± 0.04 in k_2 in cases I and II (dash-dots and dash-dot are for case I; the dashed and solid lines are for case II) for $p_L = 100$ GeV/c.

dependence. In case I, A_N decreases less with $|t|$ immediately after the maximum. But at large $|t| \geq 0.01$ GeV^2 the behaviour of A_N is very different: we can obtain a different sign for A_N at $|t| \approx 0.06$ GeV^2. In case I, when $B^-_{pC} = B^+_{pC}$, A_N changes sign in the region of $|t| \approx 0.02$ GeV^2 and then grows in magnitude. In case II, when $B^-_{pC} = 2B^+_{pC}$, A_N approaches zero and then grows positive again.

It is interesting to note that in [39], where we investigated the analysing power for the p^{12}C reaction in case I, but with a more complicated form factor, we again obtained the possibility that the slope of the hadron spin-flip exceeds the value 60 GeV^{-2}, and we showed that both slopes at very small momentum transfer were equal to about 90 GeV^{-2}. Of course, such a large slope for the spin–non-flip amplitude cannot be obtained in the standard Glauber approach and would have to come from another mechanism.

The preliminary experimental data show that A_N decreases very fast after its maximum and is almost zero in a small region of momentum transfer. This behaviour can be explained only if one assumes a negative contribution of the interference between different parts of the hadron amplitude, which changes slowly with energy. The preliminary data at $p_L = 100$ GeV/c decrease faster than those at $p_L = 24$ GeV/c, and the zero of A_N may move to lower values of $|t|$. This change of sign is independent of the normalisation of the data. It would be very interesting to obtain new data with higher accuracy and at higher energies in order to distinguish between the two scenarios for the slopes of the spin-flip amplitude.

Of course, the weak energy dependence comes from our choice of the energy dependence of the spin-flip amplitude. If we introduce, *e.g.*, an additional factor $\sqrt{s_1/s}$ with $s_1 = 6.83$ GeV (so that s_1 corresponds to $p_L = 24$ GeV/c), we obtain a strong energy dependence for A_N, which is shown in figs. 4(a), (b) in both cases, but such an energy dependence contradicts the existing experimental data. If we made the coefficient k_2 proportional to the $\rho(s)$ of the spin–non-flip amplitude, we again would obtain a strong energy dependence which is shown in figs. 5(a), (b). Hence, we can conclude that already for the present energy of proton-nucleus scattering, the part of the hadron-nucleus spin-flip amplitude connected with secondary reggeons is small and there exists a non-negligible part of the hadron-nucleus spin-flip amplitude in which the imaginary and real parts have a weak energy dependence.

4 Conclusion

By accurate measurements of the analysing power in the Coulomb-hadron interference region, we can find the structure of the hadron spin-flip amplitude, and obtain

further information about the behaviour of the hadron interaction potential at large distances. Contributions beyond the usual eikonal formalism are expected in the peripheral dynamic model [40], which takes into account hadron-hadron interactions at large distances. The resulting "residual" hadron spin-flip amplitude has a different slope from that of the spin–non-flip amplitude at small momentum transfer. The model also gives large spin effects in the diffraction dip region [41]. We should note that all our consideration are based on the usual assumption that the imaginary part of the high-energy scattering amplitude has an exponential behaviour. The other possibility, that the slope changes slowly as $t \to 0$, requires a more refined discussion that will be the subject of a subsequent paper.

O.V.S. is a Visiting Fellow of the Fonds National pour la Recherche Scientifique, Belgium. We thank V. Kanavets and D. Svirida for their comments and discussions.

References

1. C. Bourrely, J. Soffer, Nucl. Phys. B **247**, 15 (1984).
2. N. Akchurin, N.H. Buttimore, A. Penzo, Phys. Rev. D **51**, 3944 (1995).
3. O.V. Selyugin, Phys. Lett. B **333**, 245 (1994), arXiv:hep-ph/9312305.
4. A.F. Martini, E. Predazzi, Phys. Rev. D **66** , 034029 (2002).
5. A.V. Efremov, O.V. Teryaev, Phys. Lett. B **150**, 383 (1985).
6. B. Kopeliovich, M. Zaharov, Phys. Lett. B **226**, 156 (1989).
7. S.V. Goloskokov, Phys. Lett. B **315**, 459 (1993).
8. M. Anselmino, S. Forte, Phys. Rev. Lett. **71**, 223 (1993).
9. A.E. Dorokhov, N.I. Kochelev, Yu. A. Zubov, Int. J. Mod. Phys. A **8**, 603 (1993).
10. O.V. Selyugin, Phys. Rev. D **60**, 074028 (1999).
11. O.V. Selyugin, in *Proceedings of the Crimean Summer School Conference on New Trends in High Energy Physics, Crimea, 2000*, edited by P. Bogolyubov, L. Jenkovszky (Bogolyubov Institute for Theoretical Phyiscs, Kiev, 2000).
12. E. Predazzi, G. Soliani, Nuovo Cimento A **2**, 427 (1967); K. Hinotani, H.A. Neal, E. Predazzi, G. Walters, Nuovo Cimento A **52**, 363 (1979).
13. M. Sawamoto, S. Wakaizumi, Prog. Theor. Phys. **62**, 1293 (1979).
14. O.V. Selyugin, Mod. Phys. Lett. A **9**, 1207 (1994).
15. J. Schwinger, Phys. Rev. D **73**, 407 (1948).
16. B.Z. Kopeliovich, I.I. Lapidus, Sov. J. Nucl. Phys. **10**, 114 (1974).
17. N.H. Buttimore, E. Gotsman, E. Leader, Phys. Rev. D **18**, 694 (1978).
18. N. Akchurin *et al.*, Phys. Rev. D **48**, 326 (1993).
19. BNL-AGS E250 Collaboration (J. Tojo *et al.*), Phys. Rev. Lett. **89**, 052302 (2002), arXiv:hep-ex/0206057.
20. B.Z. Kopeliovich, T.L. Trueman, Phys. Rev. D **64**, 034004 (2001), arXiv:hep-ph/0012091.
21. E. Predazzi, O. Selyugin, Eur. Phys. J. A **13**, 471 (2002);
22. *Handbook of Mathematical Functions*, edited by M. Abramowitz, I. Stegun, (Dover Publ., Inc., New York 1972).
23. B. Schrempp, F. Schrempp, Nucl. Phys. B **96**, 307 (1975).
24. E. Martynov, J.R. Cudell, O.V. Selyugin, Ukr. Phys. J. **48**, 1272 (2003); hep-ph/0311019.
25. L.A. Jansen *et al.*, Nucl. Phys. A **188**, 342 (1972).
26. C.W. De Jager, H. De Vries, C. De Vries, At. Data Nucl. Data Tables **36**, 495 (1987).
27. D.R. Harrington, Phys. Rev. C **67**, 064904 (2003), arXiv:nucl-th/0206032.
28. G.G. Beznogikh *et al.*, Yad. Fiz. **18**, 348 (1973) (Sov. J. Nucl. Phys. **18**, 179 (1974)); A.A. Kuznetsov *et al.*, Yad. Fiz. **33**, 142 (1981) (Sov. J. Nucl. Phys. **33**, 74 (1981)).
29. W. Grein, Nucl. Phys. B **131**, 255 (1977); W. Grein, P. Kroll, Nucl. Phys. A **377**, 505 (1982).
30. P. Kroll, W. Schweiger, Nucl. Phys. A **503**, 865 (1989).
31. T.A. Armstrong *et al.*, Phys. Lett. B **385**, 479 (1996).
32. A. Bujak *et al.*, Phys. Rev. D **23**, 1895 (1981).
33. J.R. Cudell *et al.*, Phys. Rev. D **65** 074024 (2002), arXiv:hep-ph/0107219.
34. A. Schiz *et al.*, Phys. Rev. D **21**, 3010 (1980).
35. P.J. Karol, Phys. Rev. C **46**, 1988 (1992) .
36. P.V. Ramana Murthy, C.A. Ayre, H.R. Gustafson, L.W. Jones, M.J. Longo, Nucl. Phys. B **92**, 269 (1975).
37. SELEX Collaboration (U. Dersch *et al.*), Nucl. Phys. B **579**, 277 (2000), arXiv:hep-ex/9910052.
38. D. Svirida *et al.*, in *Proceedings ASI Symmetries and Spin, Prague, June 15-28, 2002*, to be published in Czech. J. Phys.
39. O.V. Selyugin, J.-R. Cudell, hep-ph/0301048, in *Proceedings ASI Symmetries and Spin, Prague, July 12-19, 2003*, to be published in Czech. J. Phys.
40. S.V. Goloskokov, S.P. Kuleshov, O.V. Selyugin, Z. Phys. C **50**, 455 (1991).
41. N. Akchurin, S.V. Goloskokov, O.V. Selyugin, Int. J. Mod. Phys. A **14**, 253 (1999).